Die Pharmazie

Pharmazie **2026**; 81(7): 51748
https://doi.org/10.31083/Pharmazie51748

Research Article

Investigating the Therapeutic Mechanism of *Ginkgo Biloba* Extract in Alzheimer's Disease via Integrated Network Pharmacology and Molecular Docking

Yipei LI[1,2,†], Juan GONG[3,†], Liu YANG[3], Li JIN[1,2], Ruirui PENG[2], Fang WANG[1], Li WANG[4,*]

[1]Henan Medical Key Laboratory of Neurodegenerative Diseases, Henan Medical College, 451191 Zhengzhou, Henan, China
[2]Department of Pathophysiology, School of Basic Medical Sciences, Henan Medical College, 451191 Zhengzhou, Henan, China
[3]Department of Basic Medicine, Wuxi School of Medicine, Jiangnan University, 214122 Wuxi, Jiangsu, China
[4]Clinical Medicine Science and Education Center, Faculty of Medicine, Huanghe Science and Technology College, 450061 Zhengzhou, Henan, China
*Correspondence: 202408110@hhstu.edu.cn (Li WANG)
[†]These authors contributed equally.
Academic Editor: Walter E. Müller
Submitted: 11 March 2026 Revised: 6 June 2026 Accepted: 11 June 2026 Published: 23 July 2026

Abstract

Objective: This study aimed to investigate the mechanisms through which ginkgolides in *Ginkgo biloba* extract (GBE) may protect against Alzheimer's disease (AD). **Methods:** Candidate ginkgolide constituents and their putative targets were identified using the Traditional Chinese Medicine Systems Pharmacology Database and Analysis Platform (TCMSP) and SwissTargetPrediction. AD-associated genes were retrieved from OMIM and GeneCards. Overlapping targets were used to construct component–target–disease and protein–protein interaction (PPI) networks for hub target screening. Gene Ontology (GO) and Kyoto Encyclopedia of Genes and Genomes (KEGG) enrichment analyses were performed using DAVID. AutoDock Vina was used for molecular docking, and molecular dynamics simulations were conducted to evaluate ligand–target stability. The predicted mechanisms were further examined in APP/PS1 mice and Aβ1-42-treated HT22 cells. **Results:** A total of 27 active ginkgolide-related constituents and 336 intersecting targets were identified. Ginkgolides B and M were identified as the major active compounds, whereas MAPK3, HIF-1α, and AKT1 emerged as important targets. Enrichment analysis indicated a close association with the PI3K–Akt pathway. Docking analysis showed that ginkgolides B and M bound strongly to MAPK3 and HIF-1α with binding energies ranging from –9.34 to –8.41 kcal/mol. Molecular dynamics simulations supported the stable formation of these complexes. *In vivo* and *in vitro* experiments showed that ginkgolides B and M alleviated synaptic protein damage, decreased HIF-1α expression, and improved cognitive deficits. **Conclusions:** Ginkgolides B and M may contribute to anti-AD effects in experimental models, partly through modulation of HIF-1α-related stress responses and PI3K–Akt-associated survival pathways.

Keywords: network pharmacology; Alzheimer's disease; *Ginkgo biloba* extract; molecular dynamics simulation; HIF-1α; molecular docking

1. Introduction

Alzheimer's disease (AD) represents one of the main causes of dementia in the older population. Characteristic pathological features encompass the deposition of β-amyloid (Aβ) peptides outside neurons, the formation of intraneuronal neurofibrillary tangles composed of abnormally phosphorylated tau protein, widespread neuronal degeneration, and a gradual deterioration of cognitive function [1,2]. Current therapeutic drugs mainly provide symptomatic improvement and have limited ability to delay disease progression. Adverse reactions also restrict their long-term use in some patients [3]. Although monoclonal antibodies targeting Aβ have advanced AD treatment, their clinical benefit remains limited. These findings indicate that single-target intervention is insufficient for a disorder with complex pathological networks [4]. Therefore, multicomponent natural medicines, including *Ginkgo biloba* extract (GBE), have attracted increasing interest in AD research [5].

In classic works such as the Compendium of Materia Medica, *Ginkgo biloba* has been recorded as having the effect of "nourishing the heart and brain". Modern pharmacological studies have shown that *Ginkgo biloba* possesses neuroprotective and cognition-improving activities [6]. Standardized GBE preparations, represented by EGb 761, mainly contain flavonoids and terpene lactones. Flavonoids such as quercetin, kaempferol, and luteolin account for about 22% to 27% of the extract and contribute to antioxidant and free radical scavenging effects [7,8]. Terpene lactones account for about 2.8% to 3.4% of the extract and include ginkgolides A, B, C, M, and bilobalide. These compounds participate in complex pharmacokinetic and pharmacodynamic processes and may act through complementary biological mechanisms [9]. Among them, ginkgolide B is recognized as a platelet-activating factor antagonist. It can support mitochondrial function in neural cells and reduce Aβ-related neurotoxicity [10,11,12]. Stan-

dardized *Ginkgo biloba* extracts, particularly EGb 761® and LI1370®, have been used in most pharmacological and clinical studies. According to Eckert et al. (2026) [13], these standardized extracts contain defined proportions of flavonoids, terpene lactones including ginkgolides A, B and C, and bilobalide, while potentially toxic ginkgolic acids are reduced to very low levels. Therefore, the clinical evidence for GBE mainly refers to standardized whole extracts rather than isolated ginkgolide constituents. This distinction is important for interpreting mechanistic studies using individual components such as ginkgolide B or ginkgolide M.

The active material basis and pharmacological mechanism of GBE remain difficult to clarify because multiple constituents may interact with many molecular targets. A conventional single-target strategy cannot fully explain this complex therapeutic profile. Network pharmacology provides a systems-level method for investigating multicomponent medicines [14,15]. By integrating drug components, predicted targets, disease genes, and biological pathways, this approach can reveal potential synergistic mechanisms of traditional Chinese medicine across molecular networks [16,17,18].

Ginkgo biloba leaf extract exhibits unique advantages in regulating the complex pathological network of Alzheimer's disease through its synergistic effect of multiple components. Through the integration of network pharmacology predictions and experimental validation, this study aims to explore the underlying mechanisms of GBE's "multi-target, multi-pathway" action: (1) *Ginkgo biloba* Extract exerts its therapeutic effect on Alzheimer's Disease by regulating specific target proteins; (2) The key target proteins of *Ginkgo biloba* Extract in the treatment of Alzheimer's Disease can be identified through network pharmacology, and their binding ability with the active components of *Ginkgo biloba* Extract can be verified by molecular docking; (3) The therapeutic mechanism of *Ginkgo biloba* Extract in Alzheimer's Disease is related to the regulation of the binding patterns between target proteins and active components. The study was expected to identify key active compounds, hub targets, and relevant signaling pathways, and to provide mechanistic evidence for the further development of GBE-based AD therapy.

2. Materials and Methods

2.1 Screening of Active Components and Target Identification

Candidate constituents of *Ginkgo biloba* leaves (GBLs) were retrieved from TCMSP. Compounds with oral bioavailability (OB) ≥30% and drug-likeness (DL) ≥0.18 were retained for subsequent analysis [19]. The normalized SMILES information of each selected constituent was obtained from PubChem and submitted to SwissTargetPrediction. Homo sapiens was selected as the organism, and predicted targets with probability values greater than 0.1 were included. Target information from TCMSP, SwissTargetPrediction, and GeneCards was combined. Protein names were then standardized through UniProt, followed by removal of repeated entries [20,21].

AD-related targets were searched in OMIM, DrugBank, the Therapeutic Target Database (TTD), and GeneCards by using Alzheimer's disease as the keyword [22,23,24].

2.2 Construction of the Active Component-Target Network

The intersection between GBL-related targets and AD-associated targets was identified with a Venn diagram. These genes were identified as shared targets for subsequent analysis. The common targets were uploaded to STRING to construct a protein-protein interaction (PPI) network with human as a species [25]. The active compound–shared target interaction network was constructed and visualized by Cytoscape version 3.9.1. Important nodes were identified by computing three topological metrics [26].

2.3 GO and KEGG Enrichment Analysis

Functional annotation and pathway enrichment analysis were carried out using the DAVID database (https://david.ncifcrf.gov) to explore the potential anti-AD mechanisms of GBLs. Gene Ontology (GO) enrichment analysis was performed across three domains, including molecular functions, cellular components and biological processes. Additionally, Kyoto Encyclopedia of Genes and Genomes (KEGG) pathway enrichment analysis was carried out specifically for human (Homo sapiens) target genes, with statistical significance defined as $p < 0.05$ [27,28]. The top 20 GO terms and KEGG pathways ranked by p value were visualized as bubble plots and bar charts using online bioinformatics tools (http://bioinformatics.com.cn/) [29].

2.4 Molecular Docking

The structures of ginkgolide B (GB) and ginkgolide M (GM) were downloaded from PubChem. The atomic structures of the key target proteins were retrieved from the RCSB Protein Data Bank (PDB) [30]. AutoDockTools 1.5.7 was used for hydrogen addition and charge assignment. Subsequent semi-flexible molecular docking simulations were performed using AutoDock Vina (version 1.1.2). A binding energy lower than –7 kcal/mol was regarded as evidence of strong binding affinity. PyMOL 2.5.2 was used to generate surface and three-dimensional interaction views [31]. Structural information for all target proteins used in docking is provided in Table 1.

2.5 Molecular Dynamics Simulation

All ligands and receptor proteins were protonated and ionized at physiological pH 7.4. Ligands were assigned Gasteiger charges with flexible bonds defined, where carboxyl groups were deprotonated and aliphatic amines were protonated, while hydroxyl groups were kept neutral. After removing redundant water and heteroatoms from proteins, acidic and basic amino acids were set to their corresponding charged states, and histidine was uniformly defined as the

Table 1. Structural information of target proteins used for molecular docking.

Target	PDB ID	Method	Resolution	Chains
HIF-1α	1H2K	X-RAY	2.15 Å	A
MAPK3	3FHR	X-RAY	1.90 Å	A/B
BCL2	6O0K	X-RAY	1.62 Å	A
CASP3	1GFW	X-RAY	2.80 Å	A/B
AKT1	1UNQ	X-RAY	0.98 Å	A
CCND1	2W96	X-RAY	2.30 Å	A/B
APOE	7FCR	X-RAY	1.40 Å	A
GSK3	1J1B	X-RAY	1.80 Å	A
CD4	1CDH	X-RAY	2.30 Å	A
CCL2	1DOL	X-RAY	2.40 Å	A

PDB ID, Protein Data Bank ID.

HIE form. Both optimized structures were saved as PDBQT files for molecular docking. The complexes with the most favorable docking scores were selected for 100 ns molecular dynamics simulations using GROMACS 2020. The ff14SB force field was adopted for proteins, and GAFF2 was used for the active compounds. The TIP3P model was selected for water molecules. The integration time step was set to 2 fs, and trajectory files were recorded at 20 ps intervals. Simulation trajectories were analyzed using root mean square deviation (RMSD), root mean square fluctuation (RMSF), and radius of gyration (Rg). Binding free energy was estimated with the molecular mechanics Poisson-Boltzmann surface area (MM/PBSA) method. The HIF-1α-ginkgolide M complex was analyzed using the 80 to 100 ns trajectory. The MAPK3-ginkgolide B complex was analyzed using the 50 to 100 ns trajectory. The MAPK3-ginkgolide M complex was analyzed using the 60 to 100 ns trajectory [32,33].

2.6 Animal Experiments

2.6.1 Animals and Treatment

Thirty 8-month-old male APP/PS1 double transgenic mice and ten age-matched wild-type B6C3 mice were purchased from Hangzhou Ziyuan Experimental Animal Technology Co., Ltd., Hangzhou, China. The animal production license number was SCXK (Zhejiang) 2019-0004. All mice were housed under specific pathogen-free (SPF) conditions, maintained on a 12:12 h light–dark cycle at a controlled temperature of 22 ± 2 °C and relative humidity of 50%–60%. Standard chow and water were provided ad libitum. APP/PS1 transgenic mice were randomly assigned to three groups (n = 10 per group): untreated APP/PS1 controls, APP/PS1 mice treated with GB, and APP/PS1 mice treated with GM. Age- and sex-matched wild-type (WT) littermates served as the control group. GB and GM were administered via oral gavage at a dose of 40 mg/kg twice daily [34]. The WT and APP/PS1 groups received an equal volume of normal saline. The intervention period lasted 2 months. All animal procedures followed the National Institutes of Health Guide for the Care and Use of Laboratory Animals and received approval from the Animal Ethics Committee of Jiangnan University. The approval number was JN. No20230830m0721115[329]. Prior to euthanasia via cervical dislocation, mice were deeply anesthetized by inhaling isoflurane (1.5%).

2.6.2 Fear Conditioning

For training, mice were placed in the conditioning chamber for 3 min. Three tone-foot shock pairings were then applied. The shock intensity was 0.5 mA, the shock duration was 2 s, and the interval was 58 s. After 24 h, mice were placed back into the same chamber without shock and monitored for 3 min. Freezing duration was used as an indicator of contextual memory. Behavioral data were recorded automatically using analysis software (FCT-100, Chengdu Techman, China).

2.6.3 Western Blotting

Hippocampal tissues were lysed to extract total protein, and protein concentrations were determined with the BCA method. Equal protein amounts were loaded for SDS-PAGE separation and then transferred to membranes. Membranes were incubated in a blocking solution containing 5% non-fat milk and incubated overnight at 4 °C with the primary antibodies detailed in Table 2. HRP-conjugated secondary antibodies were incubated for 1 h at room temperature. The protein bands were visualized using electrochemiluminescence. ImageJ (version 1.54f, National Institutes of Health, USA; https://imagej.nih.gov/ij/) was used for band intensity measurement, and β-actin served as the internal reference.

2.7 Cell Experiments

2.7.1 Cell Culture and Treatment

Mouse hippocampal HT22 cells were obtained from Shanghai Yihe Application Biological Technology Co., Ltd. (http://www.biowing.com.cn/). STR profiling was used for cell authentication, and mycoplasma testing showed negative results. HT22 cells were cultured in DMEM containing 10% fetal bovine serum and 1% penicillin–streptomycin at 37 °C in a humidified incubator with 5% CO_2. After stable passage, cells were exposed to 10 μM Aβ1-42 for 24 h. Treated cells then received 20 μM ginkgolide B or 20 μM ginkgolide M. For gene silencing experiments, cells were treated with siRNA targeting *HIF1A* or with a non-specific control siRNA for 48 hours [35,36]. Lipofectamine 2000 reagent was used for transfection (Thermo Fisher, TF11668019, USA). The siRNA reagents were purchased from Obio Technology Co., Ltd., Shanghai, China.

2.7.2 Real-Time Quantitative PCR and Western Blot Analysis

Total RNA and protein were isolated from cells to examine *HIF1A*, *PSD95, GluN2A*, and related genes and proteins. Primer information is presented in Table 3. Antibodies used for western blotting are shown in Table 2.

Table 2. Antibodies used for western blotting.

Antibody	Specificity	Type	Dilution for WB	Source	Catalog number
β-Actin	β-Actin	Poly-	1:5000	SAB	21338
GluN2A	NMDAR2A	Mono-	1:1000	Abcam	ab124913
PSD95	PSD95	Poly-	1:1000	CST	2507
MAPK3	ERK 1/2	Poly-	1:1000	SAB	40903
HIF-1α	Hif-1α	Recombinant antibody	1:5000	Proteintech	82989-4-RR

Mono-, monoclonal. Poly-, polyclonal; WB, Western blotting.

Table 3. PCR primers used in this study.

Gene	Forward primer(5′ → 3′)	Reverse primer(5′ → 3′)
MAPK3	ACTACCTGGACCAGCTCAAC	TAGGAAAGAGCTTGGCCCAA
AKT1	CTGCCCTTCTACAACCAGGA	CATACACATCCTGCCACACG
BCL2	CCTGGCATCTTCTCCTTCCA	CACCCCATCCCTGAAGAGTT
CCL2	CAGCCAGATGCAATCAATGCC	TGGAATCCTGAACCCACTTCT
APOE	GATCAGCTCGAGTGGCAAAG	TTGTGTGACTTGGGAGCTCT
CASP3	CAGCCAACCTCAGAGAGACA	ACAGGCCCATTTGTCCCATA
HIF1A	TGGAACATGATGGCTCCCTT	TTCTGCTGCCTTGTATGGGA
GSK3B	AGCCACTGATTACACGTCCA	CTCCTGGGGTGAAATGTCCT
CCND1	GCATGTTCGTGGCCTCTAAG	ATGGAGGGTGGGTTGGAAAT
CD4	GGCAACCTGACTCTGACTCT	CTGCTTCAGGGTCAGTCTCA

2.7.3 Immunofluorescence Staining

Cells were fixed, permeabilized, and incubated with anti-HIF1α antibody. Fluorescent secondary antibody and DAPI were then applied for signal detection and nuclear staining. Images were acquired using confocal microscopes (LSM 780, Zeiss, Germany, and LSM 880, Zeiss, Germany). Quantitative analysis of fluorescence images was performed with ImageJ software.

2.8 Statistical Analysis

To ensure robustness and reproducibility, all experiments were independently repeated at least three times per experimental group. One-way or two-way analysis of variance was performed using GraphPad Prism 9.3.1 (GraphPad Software, LLC, Boston, MA, USA). Statistical significance was defined as $p < 0.05$. Data are presented as mean ± standard error of the mean (SEM).

3. Results

3.1 Screening of Active Constituents and Network Construction

Twenty-seven active constituents of *Ginkgo biloba* were obtained from TCMSP, as listed in Table 4. Target prediction yielded 526 targets from TCMSP, 584 targets from SwissTargetPrediction, and 1442 targets from GeneCards. After target standardization and duplicate removal, 815 candidate targets were retained. These data were imported into Cytoscape 3.9.1 to generate an active constituent-target network containing 850 nodes and 1833 interactions, as presented in Fig. 1. Network topology indicated that ginkgolide B, ginkgolide M, quercetin, and luteolin were the main active constituents. The corresponding parameters are summarized in Table 5.

3.2 Identification of Core Targets and PPI Network Analysis

AD-related target collection yielded 5223 genes from GeneCards with relevance score >4203 genes from OMIM, 101 genes from TTD, and 142 genes from DrugBank. After integration and duplicate removal, 2968 AD-associated targets remained. Venn analysis revealed 336 intersecting targets between Ginkgo biloba and AD, as shown in Fig. 2A. These targets were regarded as potential therapeutic targets.

The 336 common targets were submitted to STRING for PPI network construction, as shown in Fig. 2B. Cytoscape analysis indicated that this PPI network contained 336 targets and 4413 interactions. An initial topological filter selected 80 candidate targets. Further screening with the cytoNCA plugin identified eight core targets: *MAPK3, HIF1A, AKT1, CASP3, BCL2, CD4, CCND1*, and *GSK3B*, as shown in Fig. 2C.

3.3 GO and KEGG Enrichment Analysis

GO enrichment analysis identified 839 biological process terms, 127 cellular component terms, and 247 molecular function terms. The 20 most significant GO terms are displayed in Fig. 2D, and the top 10 terms in each GO category are presented in Fig. 2E.

KEGG enrichment analysis indicated that the potential targets were associated with lipopolysaccharide response, apoptosis regulation, and inflammatory response, as shown in Fig. 2F. Pathway classification further indicated that lipid and atherosclerosis, PI3K-Akt signaling, apoptosis, and TNF signaling were enriched, as shown in Fig. 2G. The PI3K-Akt pathway contained 33 targets and showed marked enrichment. This finding suggests that PI3K-Akt

Table 4. Active compounds and ADME parameters of GBLs.

Mol ID	Molecule name	OB (%)	BBB	DL
MOL011578	Bilobalide	84.42	–1.34	0.36
MOL002680	Flavoxanthin	60.41	–0.90	0.56
MOL011586	ginkgolide B	44.38	–1.56	0.73
MOL011587	ginkgolide C	48.33	–1.76	0.73
MOL011588	ginkgolide J	44.84	–1.59	0.74
MOL011589	Ginkgolide M	49.09	–1.00	0.75
MOL011594	Isogoycyrol	40.36	0.00	0.83
MOL011597	Luteolin-4′-glucoside	41.97	–2.21	0.79
MOL011604	Syringetin	36.82	–0.59	0.37
MOL001490	bis[(2S)-2-ethylhexyl] benzene-1,2-dicarboxylate	43.59	0.68	0.35
MOL001494	Mandenol	42.00	1.14	0.19
MOL001558	sesamin	56.55	–0.08	0.83
MOL002881	Diosmetin	31.14	–0.66	0.27
MOL003044	Chryseriol	35.85	–0.53	0.27
MOL000354	isorhamnetin	49.60	–0.54	0.31
MOL000358	beta-sitosterol	36.91	0.99	0.75
MOL000422	kaempferol	41.88	–0.55	0.24
MOL000449	Stigmasterol	43.83	1.00	0.76
MOL000492	(+)-catechin	54.83	–0.73	0.24
MOL005573	Genkwanin	37.13	–0.24	0.24
MOL000006	luteolin	36.16	–0.84	0.25
MOL007179	Linolenic acid ethyl ester	46.10	1.09	0.20
MOL009278	Laricitrin	35.38	–0.69	0.34
MOL000096	(-)-catechin	49.68	–0.78	0.24
MOL000098	quercetin	46.43	–0.77	0.28
MOL002883	Ethyl oleate (NF)	32.40	1.10	0.19
MOL005043	campest-5-en-3beta-ol	37.58	0.94	0.71

ADME, absorption, distribution, metabolism, and excretion; DL, drug-likeness; GBLs, *Ginkgo biloba* leaves; OB, oral bioavailability; BBB, blood–brain barrier permeability.

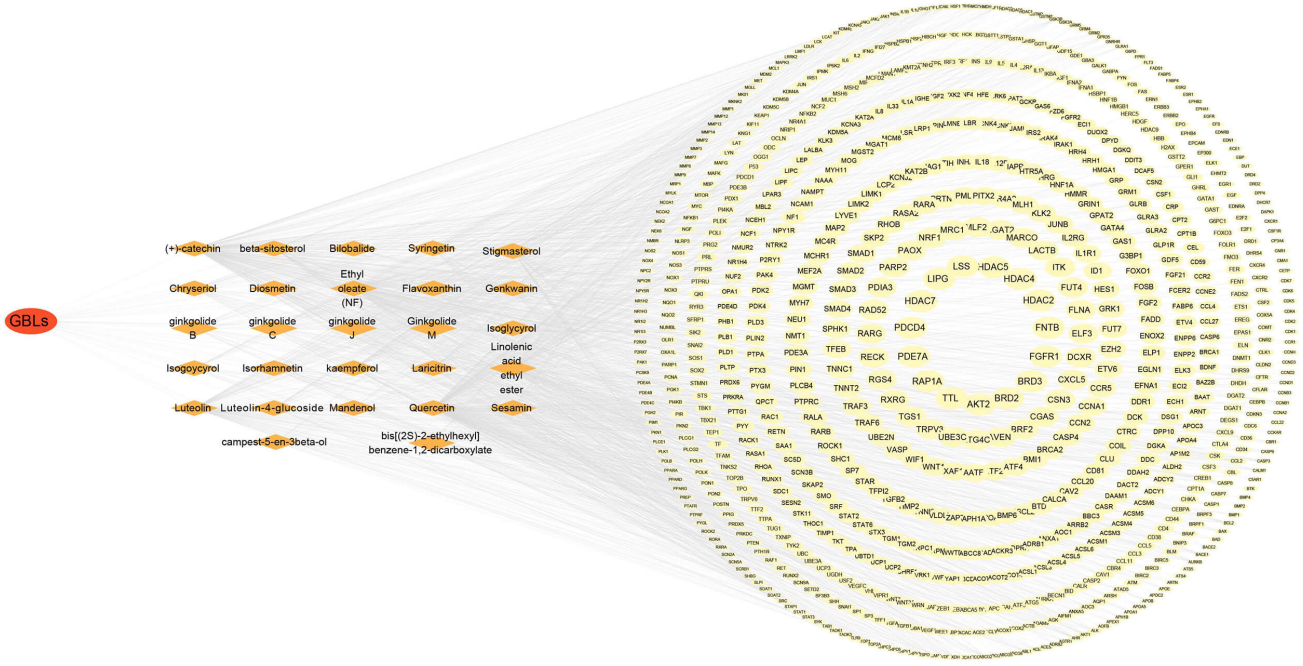

Fig. 1. Network of traditional Chinese medicine, active components, and putative targets. The red circle represents traditional Chinese medicine, orange rhombuses represent active components, and yellow circles represent candidate targets.

Table 5. Topological analysis of the active ingredient-potential targets network of GBLs.

Molecule name	Degree	Betweenness Centrality	Closeness Centrality
ginkgolide B/C/M/J	148	0.027081344	1.398918532
(+)-catechin	277	0.385670320	0.457823567
Quercetin	272	0.343206056	0.454894434
Linolenic acid ethyl ester	164	0.190609934	0.399662732
Ethyl oleate (NF)	157	0.185692571	0.396542108
Luteolin	127	0.098013230	0.383702105
beta-sitosterol	69	0.030475223	0.361097004
kaempferol	60	0.044985060	0.357825868
Stigmasterol	60	0.036884133	0.357825868
Diosmetin	49	0.006681810	0.353907417
Flavoxanthin	46	0.046431200	0.352853598
Sesamin	45	0.029123453	0.352503718
Chryseriol	43	0.005044821	0.351806037
Syringetin	41	0.004559782	0.351111111
Isorhamnetin	40	0.006955330	0.350764677
Genkwanin	39	0.008989780	0.350418926
Mandenol	36	0.028087438	0.349385749
Laricitrin	36	0.003706859	0.349385749
bis[(2S)-2-ethylhexyl] benzene-1,2-dicarboxylate	34	0.029468453	0.348700343
Luteolin-4′-glucoside	30	0.009533734	0.347337567
Isoglycyrol	25	0.016057311	0.345649003
campest-5-en-3beta-ol	21	0.001818680	0.344309927
Bilobalide	11	0.003668552	0.341007194
Isogoycyrol	3	0.002814639	0.338410281

GBLs, *Ginkgo biloba* leaves.

signaling may be an important pathway involved in the anti-AD activity of Ginkgo biloba.

3.4 Molecular Docking and Molecular Dynamics Simulation

The 10 highest-ranked target proteins were selected according to degree, closeness, and betweenness centrality values, as shown in Fig. 3A. Docking analysis of the 12 active components with these targets revealed that ginkgolide M had the strongest affinity for MAPK3 with a binding energy of –9.34 kcal/mol. Ginkgolide B bound well to MAPK3 with a binding energy of –9.18 kcal/mol. In addition, ginkgolide M bound to HIF-1α with a binding energy of –8.41 kcal/mol, as shown in Fig. 3B. 2D chemical structures of GB and GM were shown in Fig. 3C. Docking and molecular dynamics analysis indicated that ginkgolides could form stable binding conformations with HIF-1α and MAPK3. Ginkgolide M formed hydrogen bonds with Lys310 and Glu261 of HIF-1α. Interactions with Pro240 and Glu334 were observed in the MAPK3-ginkgolide M complex. Ginkgolide B occupied the ATP-binding pocket of MAPK3 and interacted with Glu131 and Lys325, as shown in Fig. 3D–F. All three ligands were embedded in deep receptor cavities and showed good shape complementarity. These results suggested that HIF-1αmay be a candidate molecular target associated with the protective effects of GB and GM in the present experimental models.

The RMSD curve reflects variations in the protein structure. An RMSD value below 0.2 nm indicates that the molecular conformation undergoes no significant changes and tends toward stability. After the 100 ns molecular dynamics simulation, HIF-1α-ginkgolide M, and MAPK3-ginkgolide M tended to be smooth after 0, and 20 ns, respectively. However, the RMSD curve of the MAPK3-ginkgolide B fluctuated continuously within a narrow range (Fig. 4A). The results indicated that the binding of HIF-1α-ginkgolide M and MAPK3-ginkgolide M to the receptor protein does not induce a persistent and substantial alteration in their conformation, and that the HIF-1α-ginkgolide M complex is comparatively stable. The tiny molecule forms a stable, tightly bound complex with the protein, as confirmed by the RMSF curve indicating fluctuations in the amino acid residues of the protein. The RMSF curve for HIF-1α-ginkgolide M, MAPK3-ginkgolide B, and MAPK3-ginkgolide M demonstrated that the intermediate portions of the proteins exhibited reduced residue flexibility compared to other regions, indicating that these areas served as molecular binding sites or secondary structures, thus possessing greater stability (Fig. 4B). The RG curve reflects the compactness of the entire protein structure. The results indicated that all compounds exhibited stable gyration radii (Fig. 4C). The SASA curve indirectly reflects the tightness of protein wrapped ligand. The result showed that the exposure of ligands to solvent in the

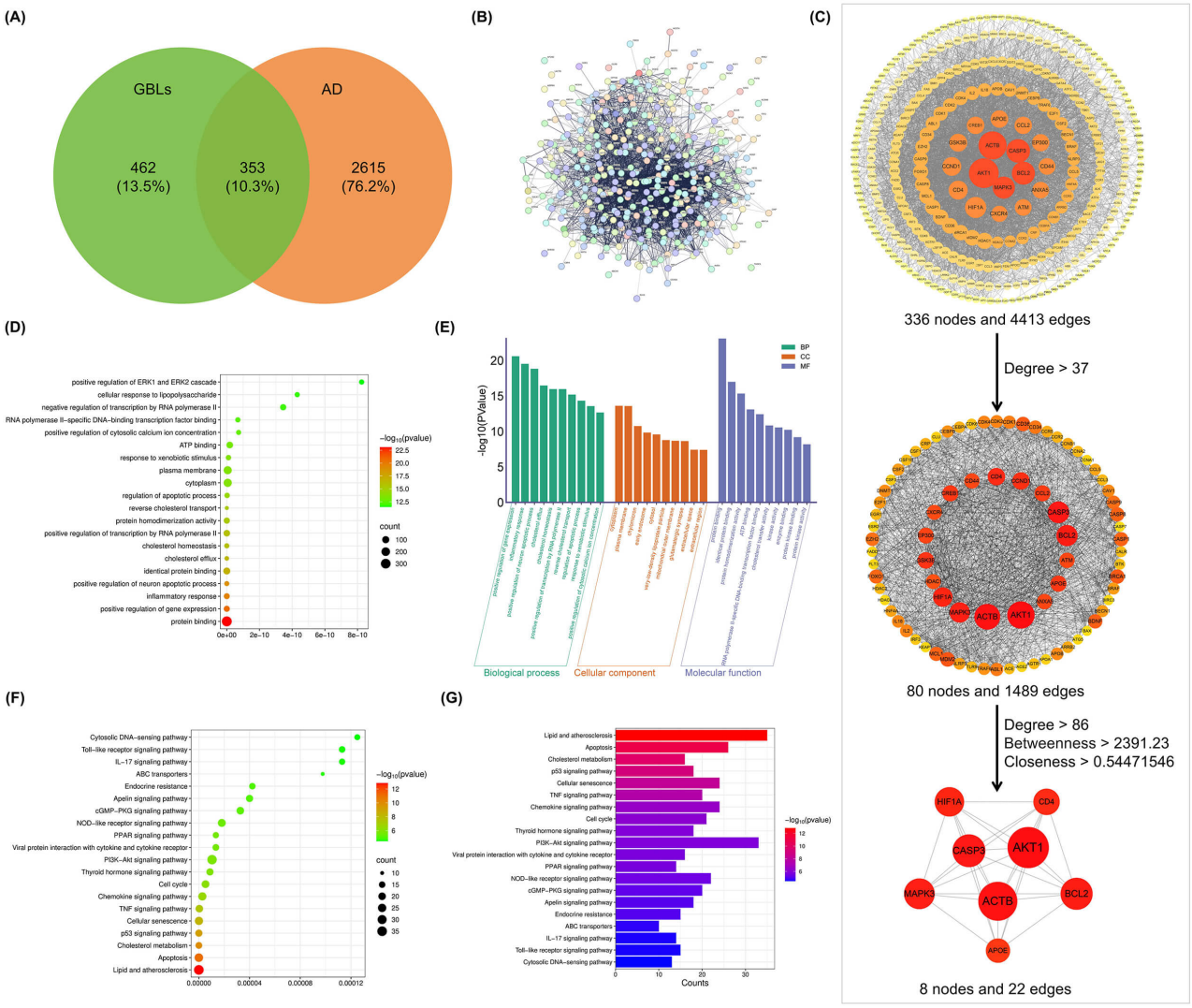

Fig. 2. Network and enrichment analysis. (A) Venn diagram showing shared targets between GBLs and AD. (B) PPI network of potential therapeutic targets. Edge color and size indicate BC, CC, and DC values. (C) Screening workflow for key targets. Red nodes represent the eight core targets. (D) GO enrichment bubble plot. (E) GO enrichment bar plot. (F) KEGG enrichment bubble plot. (G) KEGG pathway classification. AD, Alzheimer's disease; PPI, protein-protein interaction; BC, betweenness centrality; CC, closeness centrality; DC, degree centrality; GO, Gene Ontology; KEGG, Kyoto Encyclopedia of Genes and Genomes.

combinations are relatively small. And the exposure of ginkgolide M to solvent in the HIF1A-ginkgolide M combination is the least, which demonstrates that HIF-1α wrapped ginkgolide M more tightly (Fig. 4D). The Number of H-bond reflects the combination tightness between protein and ligand. HIF-1α-ginkgolide M, MAPK3-ginkgolide B, and MAPK3-ginkgolide M form stably 2 hydrogen bonds, occasionally reaching a maximum of 5 (Fig. 4E).

The above results imply that these ligand-protein complexes are stable and tightly folded, and the binding of HIF-1α-ginkgolide M is the tightest. Consequently, it may be inferred that the stability of these complexes is not influenced by small molecule binding.

The binding free energies between small molecules and proteins were computed using the MM/PBSA equation, utilizing 80–100 ns trajectories for HIF-1α-ginkgolide M, 50–100 ns trajectories for MAPK3-ginkgolide B, and 60–100 ns trajectories for MAPK3-ginkgolide M. MM/PBSA analysis showed binding free energies of –48.008, –20.262, and –48.617kJ/mol for HIF-1α-ginkgolide M, MAPK3-ginkgolide B, and MAPK3-ginkgolide M, as shown in Table 6 [33]. Van der Waals and electrostatic forces played key roles in promoting binding between the small molecules and proteins in all three cases. The van der Waals energy is the predominant contributor to the binding energy. The MAPK3-ginkgolide M complex has the highest binding free energy, followed by the HIF-1α-ginkgolide M and MAPK3-ginkgolide B complexes (Fig. 5A–C). Through residue specific binding free energy decomposition, residues in each complex that have the most positive impact on binding stability were identified (Fig. 5D–F). In summary, ginkgolide M and ginkgolide B formed sta-

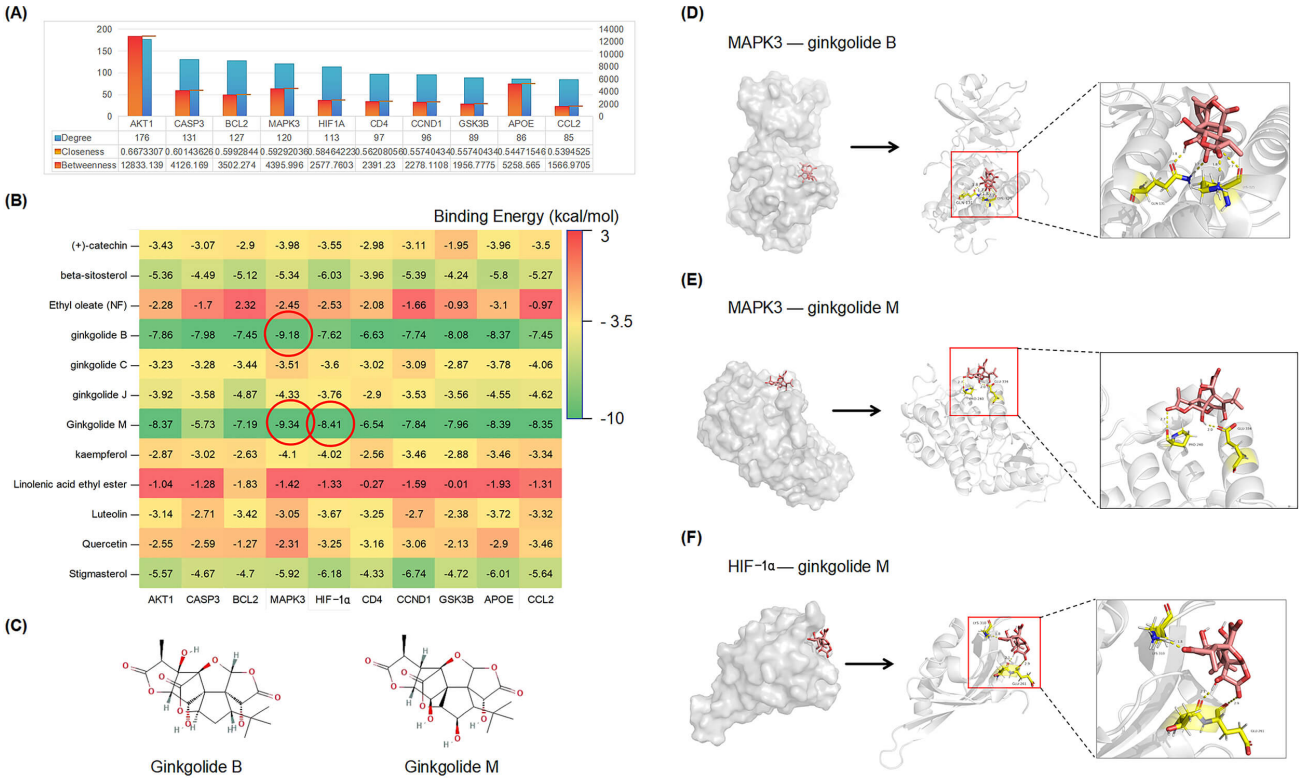

Fig. 3. Core target screening and molecular docking analysis of active constituents from Ginkgo biloba. (A) Bar plot of the 10 key targets ranked by degree, closeness, and betweenness values. (B) Heat map of docking binding energy. Lower values indicate stronger binding affinity. (C) 2D chemical structures of GB and GM. (D) MAPK3-ginkgolide B docking model. (E) MAPK3-ginkgolide M docking model. (F) HIF-1α-ginkgolide M docking model. GB, ginkgolide B; GM, ginkgolide M.

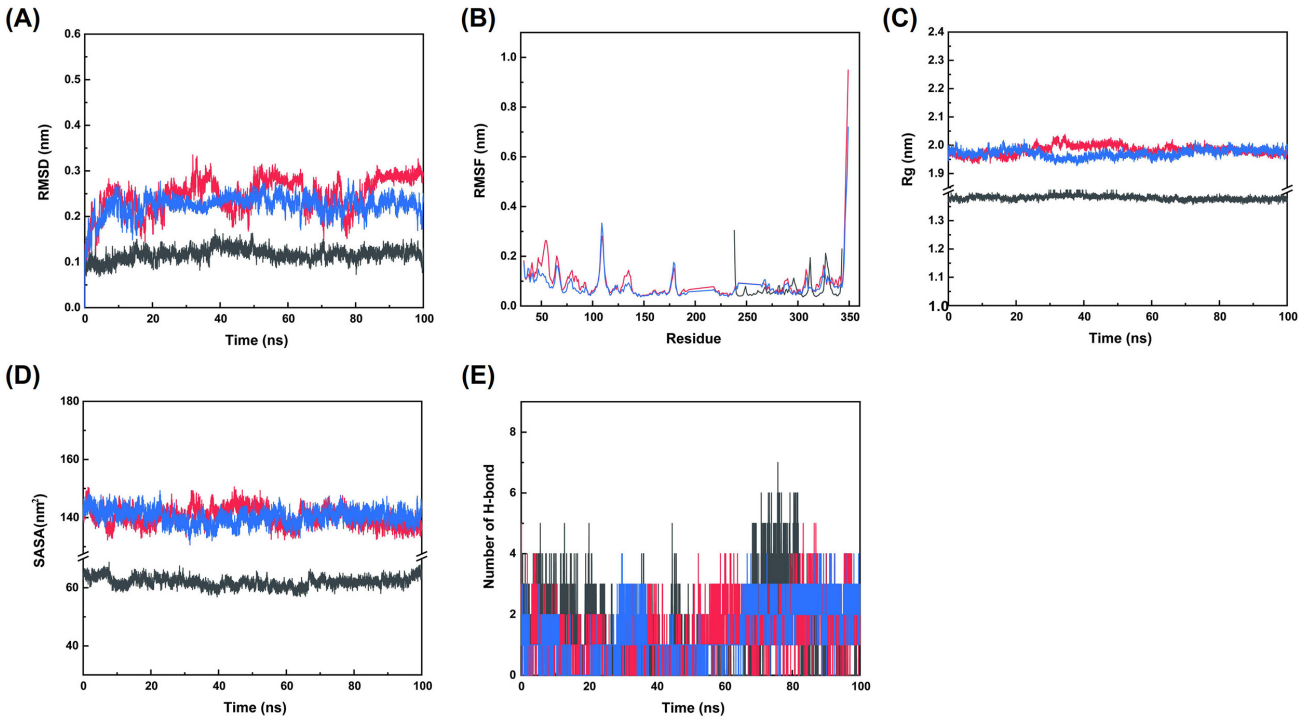

Fig. 4. Molecular dynamics simulation analysis. (A) RMSD curves. (B) RMSF curves. (C) Radius of gyration curves. (D,E) Solvent accessible surface area curves and hydrogen bond numbers for ligand-protein complexes. The black curve represents HIF-1α-ginkgolide M, the red curve is MAPK3-ginkgolide B, and the blue curve is MAPK3-ginkgolide M. RMSD, root mean square deviation; RMSF, root mean square fluctuation; Rg, radius of gyration; SASA, solvent-accessible surface area.

Table 6. Free energy and components of combined molecular dynamics simulations.

Energy component (kJ/mol)	HIF-1α-ginkgolide M	MAPK3-ginkgolide B	MAPK3-ginkgolide M
VDWAALS	–62.033	–95.289	–77.800
EEL	–3.301	–28.988	–118.063
EGB	28.322	119.483	161.564
ESURF	–10.996	–15.468	–14.318
Total Binding Energy	–48.008	–20.262	–48.617

VDWAALS, van der Waals energy; EEL, electrostatic energy; EGB, polar solvation energy; ESURF, non-polar solvation energy.

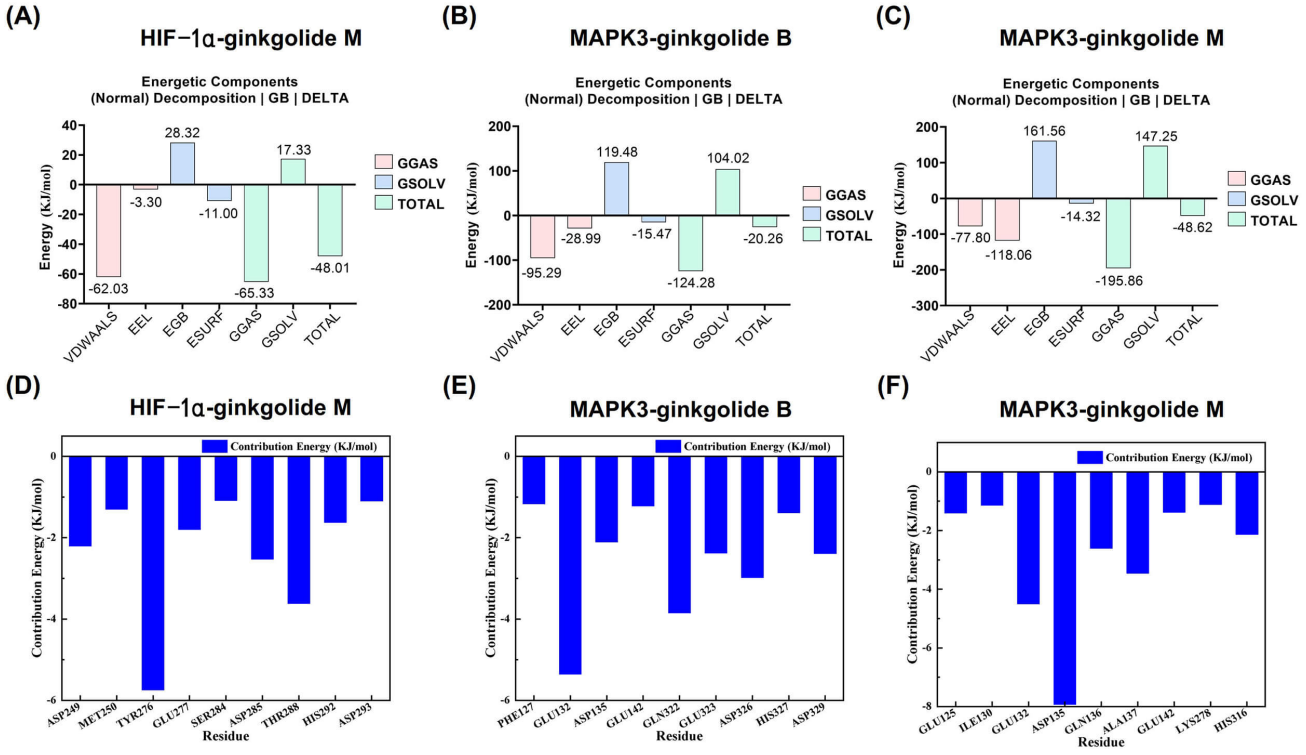

Fig. 5. MM/PBSA analysis of ginkgolide-target complexes. (A–C) Energy components of the complexes, including VDWAALS, EEL, EGB, ESURF, GGAS, GSOLV, and TOTAL. GGAS equals VDWAALS plus EEL. GSOLV equals EGB plus ESURF. TOTAL equals GGAS plus GSOLV. (D–F) Residue energy contributions related to binding stability. MM/PBSA, molecular mechanics Poisson-Boltzmann surface area.

ble complexes with key targets of MAPK3 and HIF-1α, and maintained strong binding affinity and stability. These results provide a molecular basis for the potential therapeutic effect of ginkgolide B and ginkgolide M in AD.

3.5 Experimental Validation in Animals and Cells

APP/PS1 mice were treated with ginkgolide B (GB) or ginkgolide M (GM) by gavage for 2 months. In the contextual fear conditioning test, APP/PS1 mice exhibited reduced freezing behavior compared with WT mice. GB and GM treatment increased freezing duration, as shown in Fig. 6A,B. Western blotting showed elevated HIF-1αand MAPK expression and reduced GluN2A and PSD95 expression in the hippocampus of APP/PS1 mice. GB and GM treatment partially reversed these protein changes, as shown in Fig. 6C,D. Similar protective effects were observed in HT22 cells. RT-qPCR results showed that GB or GM reduced the mRNA levels of *BCL2, MAPK, HIF1A, CCND1, APOE,* and *CCL2* in Aβ-injured cells, as shown in Fig. 6E. Immunofluorescence analysis showed marked HIF1A accumulation after Aβ exposure, while GB and GM reduced the HIF1A signal, as shown in Fig. 6F,G. *HIF1A* knockdown also attenuated the Aβ-induced reduction in PSD95 and GluN2A, as shown in Fig. 6H,I. These findings support HIF-1α as an important target involved in the neuroprotective action of ginkgolides.

4. Discussion

To elucidate the potential mechanisms underlying the effects of *Ginkgo biloba* extract (GBE) in Alzheimer's disease (AD), the present study combined network pharmacology, molecular docking, molecular dynamics simulations, and experimental validation. Ginkgolides B and

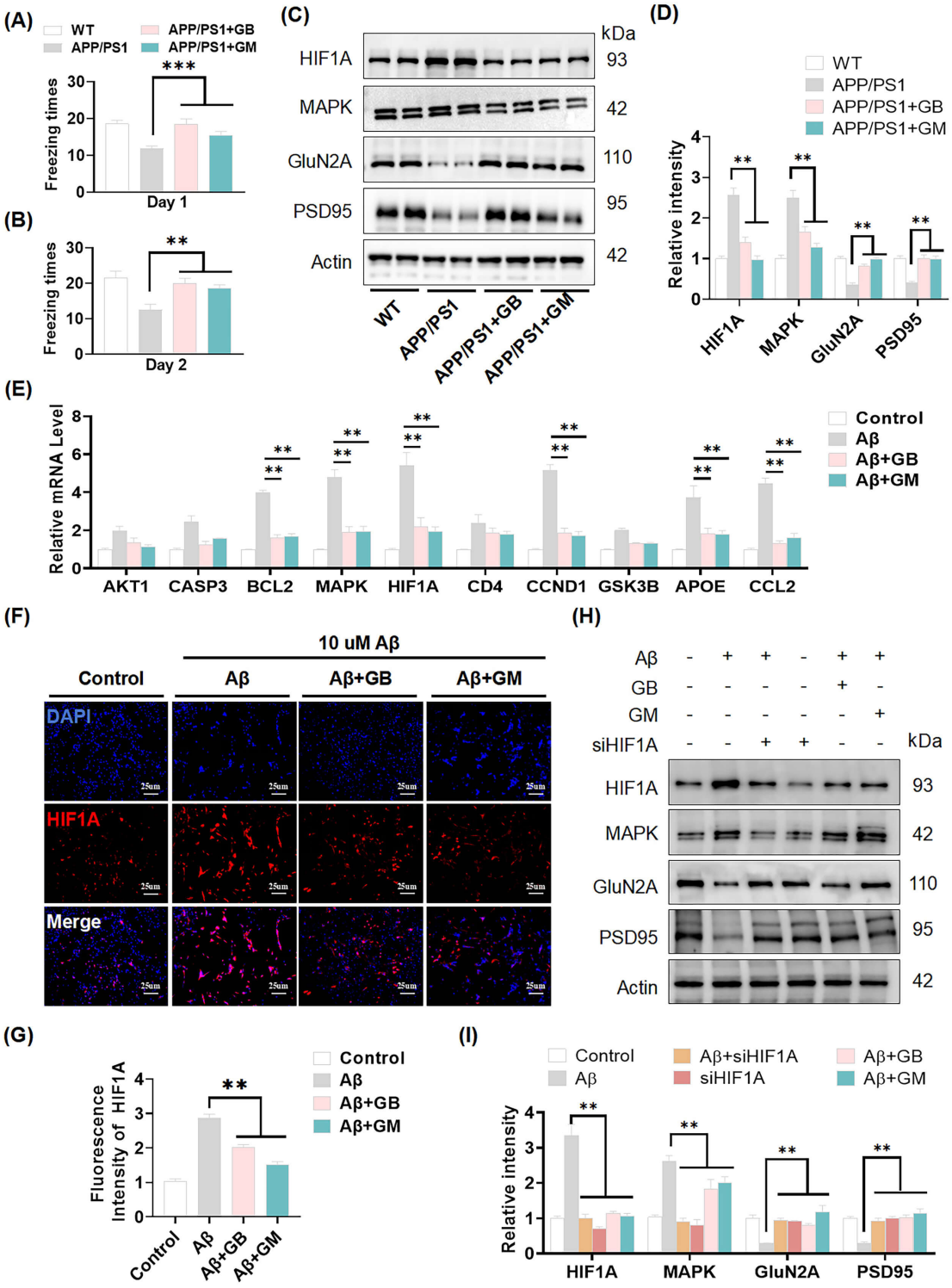

Fig. 6. Effects of ginkgolides B and M on key targets and neuroprotection in animals and cells. (A,B) Freezing behavior in the four mouse groups after fear conditioning. (C,D) Western blotting and quantitative analysis of HIF-1α, MAPK, GluN2A, and PSD95 in hippocampus, n = 4. (E) RT-qPCR analysis of the 10 selected targets in HT22 cells, n = 4. (F,G) Representative HIF1A immunofluorescence images in HT22 cells, n = 3. Scale bar = 25 μm. (H,I) Western blotting of HIF-1α, MAPK, GluN2A, and PSD95 in HT22 cells, n = 3 per group. Each experiment was repeated at least three times. Data are shown as mean ± SEM. $^{**}p < 0.01$, $^{***}p < 0.001$ versus the APP/PS1 group (panels A, B, D) and versus the Aβ group (panels E, G, I). Data in A, B, and G were analyzed by one-way ANOVA with Bonferroni post hoc test. Data in D, E, and I were analyzed by two-way ANOVA with Bonferroni post hoc test. RT-qPCR, Real-time quantitative polymerase chain reaction; SEM, standard error of the mean; Aβ, β-amyloid; ANOVA, Analysis of variance.

M were identified as important constituents derived from *Ginkgo biloba* leaves associated with AD-related targets. In APP/PS1 mice, treatment with ginkgolide B or ginkgolide M improved contextual fear memory and partially restored synaptic protein expression. In Aβ1–42-treated HT22 cells, both compounds attenuated Aβ-induced injury and reduced HIF-1α overexpression. These findings suggest that ginkgolides B and M may contribute to neuroprotective effects in AD-related experimental models.

Ginkgolide B is a known platelet-activating factor receptor antagonist with anti-inflammatory, antioxidant, and anti-apoptotic properties [37,38]. Ginkgolide M has been less extensively investigated. Available evidence suggests that ginkgolide M may also possess neuroprotective and free radical-scavenging activities [39,40]. The present results extend these observations by showing that both ginkgolide B and M regulate stress-related and synaptic proteins in AD models. Nevertheless, these findings require caution, as most pharmacological and clinical evidence for GBE is derived from standardized whole extracts (e.g., EGb 761®), not from isolated ginkgolides.

The predicted target activities should therefore be discussed in the context of established pharmacological and clinical data for standardized GBE. Eckert et al. (2005) [5] emphasized that the neuroprotective activity of standardized GBE is mainly associated with antioxidant effects, improvement of mitochondrial function, stabilization of mitochondrial membrane potential, restoration of neuronal energy metabolism, support of neuroplasticity, and reduction of neuroinflammation. These mechanisms align with earlier pharmacological studies showing that EGb 761 improves mitochondrial membrane potential and neuronal energy metabolism, and that GBE rescues Aβ-induced impairment of oxidative phosphorylation [41]. Thus, the overall pharmacological background of GBE supports the biological plausibility of mechanisms involving oxidative stress, mitochondrial dysfunction, neuronal survival, and synaptic plasticity.

Within this framework, the identification of HIF-1α, MAPK3, and PI3K-Akt-related signaling in our network analysis is pharmacologically plausible, but should not be overinterpreted as direct clinical target validation. HIF-1α is a stress-responsive transcription factor involved in hypoxia, oxidative stress, inflammatory responses, and metabolic adaptation [42]. In the present study, Aβ exposure increased HIF-1α expression, whereas ginkgolide B and M reduced this overexpression in both animal and cellular models. This finding is consistent with the reported ability of GBE to alleviate oxidative and mitochondrial stress [43,44]. However, currently available clinical data for standardized GBE do not directly demonstrate HIF-1α modulation in patients with AD or mild cognitive impairment. Therefore, HIF-1α should be regarded as an experimentally supported candidate target in our models, rather than a clinically validated pharmacodynamic target of GBE.

MAPK3 and PI3K-Akt signaling are also relevant to neuronal survival, stress responses, and synaptic plasticity. The PI3K-Akt pathway regulates cell survival, metabolism, and synaptic function, and its impairment is associated with AD-related pathology [45,46]. Previous pharmacological work showed that standardized GBE can increase neurite outgrowth and activate the Akt/mTOR pathway in neuronal models [8]. This supports the biological relevance of the PI3K-Akt enrichment observed in our network analysis. However, this evidence was obtained mainly with standardized GBE as a whole extract, whereas our experimental validation focused on ginkgolides B and M. Therefore, our results suggest that ginkgolides B and M may participate in, but do not fully represent, the multi-component and multi-target activity of standardized GBE.

The synaptic findings further support these mechanisms. GluN2A is an essential NMDA receptor subunit involved in synaptic transmission, whereas PSD95 is a key scaffold protein required for synaptic structure and function. Reduced expression of GluN2A and PSD95 is closely associated with synaptic impairment in AD [47]. In the present study, APP/PS1 mice and Aβ-treated HT22 cells showed reduced GluN2A and PSD95 expression, while treatment with ginkgolide B or M partially restored these proteins. *HIF1A* knockdown also attenuated the Aβ-induced reduction of PSD95 and GluN2A, suggesting that excessive HIF-1α activation contributes to Aβ-associated synaptic injury. Together, these results indicate that ginkgolides B and M may protect synaptic function partly by modulating HIF-1α-related stress responses and PI3K-Akt-associated survival pathways.

From a clinical perspective, randomized and controlled studies of standardized EGb 761 have reported benefits in cognitive and functional outcomes in AD or vascular dementia patients [7]. These clinical data support the therapeutic plausibility of GBE in age-related neurocognitive disorders. However, they do not directly validate HIF-1α, MAPK3, or PI3K-Akt signaling as patient-level pharmacodynamic biomarkers. Moreover, because clinical studies generally evaluated standardized GBE as a whole extract, clinical benefits cannot be directly attributed to ginkgolide B or ginkgolide M alone. The present findings therefore provide a mechanistic link between computational prediction and experimental validation, but further studies using standardized GBE, isolated constituents, target-specific interventions, and clinically relevant biomarkers are required.

In conclusion, the present study suggests that ginkgolides B and M exert neuroprotective effects in AD-related experimental models. These effects may involve attenuation of Aβ-induced HIF-1α overexpression, modulation of PI3K-Akt-related survival signaling, and restoration of synaptic proteins including GluN2A and PSD95. These mechanisms are consistent with the broader pharmacological profile of standardized GBE, particularly its antioxidant, mitochondrial protective, and neuroplasticity-supporting actions. However, HIF-1α, MAPK3, and PI3K-

Akt should currently be considered candidate mechanistic targets rather than clinically validated targets of GBE. Further experimental and translational studies are needed to determine whether these targets are directly involved in the clinical effects of standardized GBE in AD and related neurocognitive disorders.

5. Limitations

Several limitations should be noted. First, screening of active components relied on TCMSP and SwissTargetPrediction. Some active metabolites formed *in vivo* may therefore have been missed. Second, molecular dynamics simulation supported stable binding of ginkgolides B and M to MAPK3 and HIF-1α, but the simulation did not capture the full brain microenvironment. Factors such as other biomolecules, pH changes, and signaling cross-talk were not included. Third, the study focused mainly on HIF-1α and the PI3K-Akt pathway. Interactions among different ginkgolide components were not examined in depth. Future studies might be needed to explore the therapeutic mechanism of ginkgolides in AD more clearly. Fourth, although the present study identified HIF-1α, MAPK3, and PI3K-Akt-related signaling as potential mechanisms of ginkgolides B and M, the available clinical evidence mainly concerns standardized GBE/EGb 761 as a whole extract. These clinical studies did not directly measure HIF-1α, MAPK3, or PI3K-Akt activity as pharmacodynamic biomarkers. Therefore, the clinical relevance of these predicted and experimentally observed targets remains to be further validated. Future studies should examine whether modulation of these targets occurs after standardized GBE treatment in AD models and, if possible, in patient-derived samples.

6. Conclusions

In summary, ginkgolides B and M in Ginkgo biloba extract may act against AD by targeting proteins such as HIF-1α and MAPK3 and by regulating the PI3K-Akt pathway. These effects may reduce synaptic injury and help preserve neuronal function. The findings support the multicomponent and multitarget characteristics of Ginkgo biloba extract in AD intervention and provide evidence for its further precise clinical development.

Availability of Data and Materials

Datasets supporting this study are available from the corresponding author upon request.

Author Contributions

Conceptualization, YPL, JG and LW; Formal analysis, JG, LY, LJ and LW; Investigation, YPL, JG, RRP, and FW; Methodology, JG and LY; Project administration and Resources, YPL and LW; Supervision, YPL and LW; Validation, YPL and JG; Visualization, YPL and JG; Writing-original draft, YP. All authors contributed to editorial changes in the manuscript. All authors have participated sufficiently in the work and agreed to be accountable for all aspects of the work. All authors read and approved the final manuscript.

Ethics Approval and Consent to Participate

The animal study was approved by the Animal Ethics Committee of Jiangnan University (Approval No. JN. No20230830m0721115[329]). All animal procedures were performed in accordance with the National Institutes of Health Guide for the Care and Use of Laboratory Animals. The ARRIVE guidelines were also followed to ensure transparent reporting of the in vivo experiments.

Acknowledgment

The authors acknowledge Henan Medical College and Jiangnan University for providing the research assistance.

Funding

This work was supported by the Scientific and Technological Project in Henan Province (Grant No. 232102311152). The funder had no role in the study design, data collection, data analysis, data interpretation, or manuscript writing.

Conflicts of Interest

The authors declare that they have no known competing financial interests or personal relationships that could have appeared to influence the work reported in this paper.

Supplementary Material

Supplementary material associated with this article can be found, in the online version, at https://doi.org/10.31083/Pharmazie51748.

References

[1] Scheltens P, De Strooper B, Kivipelto M, Holstege H, Chételat G, Teunissen CE, et al. Alzheimer's disease. Lancet (London, England). 2021; 397: 1577–1590. https://doi.org/10.1016/S0140-6736(20)32205-4

[2] Inoue Y, Shue F, Bu G, Kanekiyo T. Pathophysiology and probable etiology of cerebral small vessel disease in vascular dementia and Alzheimer's disease. Molecular Neurodegeneration. 2023; 18: 46. https://doi.org/10.1186/s13024-023-00640-5

[3] Breijyeh Z, Karaman R. Comprehensive Review on Alzheimer's Disease: Causes and Treatment. Molecules (Basel, Switzerland). 2020; 25: 5789. https://doi.org/10.3390/molecules25245789

[4] Ali J, Choe K, Park JS, Park HY, Kang H, Park TJ, et al. The Interplay of Protein Aggregation, Genetics, and Oxidative Stress in Alzheimer's Disease: Role for Natural Antioxidants and Immunotherapeutics. Antioxidants (Basel, Switzerland). 2024; 13: 862. https://doi.org/10.3390/antiox13070862

[5] Eckert A, Keil U, Scherping I, Hauptmann S, Müller WE. Stabilization of mitochondrial membrane potential and improvement of neuronal energy metabolism by Ginkgo biloba extract EGb 761. Annals of the New York Academy of Sciences. 2005; 1056: 474–485. https://doi.org/10.1196/annals.1352.023

[6] Liu Y, Xin H, Zhang Y, Che F, Shen N, Cui Y. Leaves, seeds and exocarp of Ginkgo biloba L. (Ginkgoaceae): A Comprehensive Review of Traditional Uses, phytochemistry, pharmacology, resource utilization and toxicity. Journal of Ethnopharmacology. 2022; 298: 115645. https://doi.org/10.1016/j.jep.2022.115645

[7] Budeč M, Bošnir J, Racz A, Lasić Study Group D, Brkić D, Mosović Ćuić A. VERIFICATION OF AUTHENTICITY OF *GINKGO BILOBA* L. LEAF EXTRACT AND ITS PRODUCTS PRESENT ON THE CROATIAN MARKET BY ANALYSIS OF QUANTITY AND RATIO OF GINKGO FLAVONE GLYCOSIDES (QUERCETIN, KAEMPFEROL AND ISORHAMNETIN) TO TERPENE TRILACTONES TO THE EFFECT OF UNMASKING COUNTERFEIT DRUGS ENDANGERING PATIENT HEALTH. Acta Clinica Croatica. 2019; 58: 672–692. https://doi.org/10.20471/acc.2019.58.04.15

[8] Lejri I, Grimm A, Eckert A. Ginkgo biloba extract increases neurite outgrowth and activates the Akt/mTOR pathway. PLoS ONE. 2019; 14: e0225761. https://doi.org/10.1371/journal.pone.0225761

[9] Zhang L, Fang X, Sun J, Su E, Cao F, Zhao L. Study on Synergistic Anti-Inflammatory Effect of Typical Functional Components of Extracts of Ginkgo Biloba Leaves. Molecules (Basel, Switzerland). 2023; 28: 1377. https://doi.org/10.3390/molecules28031377

[10] Ye W, Wang J, Little PJ, Zou J, Zheng Z, Lu J, et al. Anti-atherosclerotic effects and molecular targets of ginkgolide B from *Ginkgo biloba*. Acta Pharmaceutica Sinica. B. 2024; 14: 1–19. https://doi.org/10.1016/j.apsb.2023.09.014

[11] Wu T, Li D, Chen Q, Kong D, Zhu H, Zhou H, et al. Identification of VDAC1 as a cardioprotective target of Ginkgolide B. Chemico-Biological Interactions. 2025; 406: 111358. https://doi.org/10.1016/j.cbi.2024.111358

[12] Liu GZ, Niu TT, Yu Q, Xu BL, Li XQ, Yuan BY, et al. Ginkgolide attenuates memory impairment and neuroinflammation by suppressing the NLRP3/caspase-1 pathway in Alzheimer's disease. Aging. 2023; 15: 10237–10252. https://doi.org/10.18632/aging.205072

[13] Eckert A, Georgescu D, Seifritz E, Müller WE. Improvement of age-related neurocognitive disorders by Ginkgo biloba extract: neuroprotection in focus. International Journal of Psychiatry in Clinical Practice. 2026; 30: 115–128. https://doi.org/10.1080/13651501.2026.2617217

[14] Pan J, Tang J, Gai J, Jin Y, Tang B, Fan X. Exploring the mechanism of Ginkgo biloba L. leaves in the treatment of vascular dementia based on network pharmacology, molecular docking, and molecular dynamics simulation. Medicine. 2023; 102: e33877. https://doi.org/10.1097/MD.0000000000033877

[15] Zhou J, Qian M, Li C, Zhou W, Yao L, Chen Y, et al. Metabolomics and integrated network pharmacology analysis reveal that ginkgolides act as potential active anticancer components by regulating one-carbon metabolism. Journal of Ethnopharmacology. 2022; 298: 115609. https://doi.org/10.1016/j.jep.2022.115609

[16] Zhang P, Zhang D, Zhou W, Wang L, Wang B, Zhang T, et al. Network pharmacology: towards the artificial intelligence-based precision traditional Chinese medicine. Briefings in Bioinformatics. 2023; 25: bbad518. https://doi.org/10.1093/bib/bbad518

[17] Nogales C, Mamdouh ZM, List M, Kiel C, Casas AI, Schmidt HHHW. Network pharmacology: curing causal mechanisms instead of treating symptoms. Trends in Pharmacological Sciences. 2022; 43: 136–150. https://doi.org/10.1016/j.tips.2021.11.004

[18] Jin R, Zhao Z, Zhang Q, Sun YU, Wang W, Peng D. An anti-inflammatory active ingredients in *Poriae cutis*: Screening based on network pharmacology. Die Pharmazie. 2024; 79: 72–81. https://doi.org/10.1691/ph.2024.3647

[19] Xiang C, Liao Y, Chen Z, Xiao B, Zhao Z, Li A, et al. Network Pharmacology and Molecular Docking to Elucidate the Potential Mechanism of Ligusticum Chuanxiong Against Osteoarthritis. Frontiers in Pharmacology. 2022; 13: 854215. https://doi.org/10.3389/fphar.2022.854215

[20] Daina A, Michielin O, Zoete V. SwissTargetPrediction: updated data and new features for efficient prediction of protein targets of small molecules. Nucleic Acids Research. 2019; 47: W357–W364. https://doi.org/10.1093/nar/gkz382

[21] Pichler K, Warner K, Magrane M, UniProt Consortium. SPIN: Submitting Sequences Determined at Protein Level to UniProt. Current Protocols in Bioinformatics. 2018; 62: e52. https://doi.org/10.1002/cpbi.52

[22] Amberger JS, Hamosh A. Searching Online Mendelian Inheritance in Man (OMIM): A Knowledgebase of Human Genes and Genetic Phenotypes. Current Protocols in Bioinformatics. 2017; 58: 1.2.1–1.2.12. https://doi.org/10.1002/cpbi.27

[23] Marbán-González A, Ramírez-Cid V, Cristóbal-Ramírez A, Medina-Franco JL. Exploiting PubChem and other public databases for virtual screening in 2025: what are the latest trends? Expert Opinion on Drug Discovery. 2025; 20: 1387–1403. https://doi.org/10.1080/17460441.2025.2558161

[24] Zhou Y, Zhang Y, Zhao D, Yu X, Shen X, Zhou Y, et al. TTD: Therapeutic Target Database describing target druggability information. Nucleic Acids Research. 2024; 52: D1465–D1477. https://doi.org/10.1093/nar/gkad751

[25] Ullanat V, Jing B, Sledzieski S, Berger B. Learning the language of protein-protein interactions. Nature Communications. 2026; 17: 1199. https://doi.org/10.1038/s41467-025-67971-3

[26] Dubchenko EA, Ivanov AV, Boiko AN, Spirina NN, Gusev EI, Kubatiev AA. Hyperhomocysteinemia and endothelial dysfunction in patients with cerebral vascular and autoimmune diseases. Zhurnal Nevrologii i Psikhiatrii Imeni S.S. Korsakova. 2019; 119: 133–138. https://doi.org/10.17116/jnevro2019119111133

[27] Sherman BT, Panzade G, Imamichi T, Chang W. DAVID Ortholog: an integrative tool to enhance functional analysis through orthologs. Bioinformatics (Oxford, England). 2024; 40: btae615. https://doi.org/10.1093/bioinformatics/btae615

[28] Chen L, Zhang YH, Wang S, Zhang Y, Huang T, Cai YD. Prediction and analysis of essential genes using the enrichments of gene ontology and KEGG pathways. PLoS ONE. 2017; 12: e0184129. https://doi.org/10.1371/journal.pone.0184129

[29] Di H, Liu H, Xu S, Yi N, Wei G. Network Pharmacology and Experimental Validation to Explore the Molecular Mechanisms of Compound Huangbai Liquid for the Treatment of Acne. Drug Design, Development and Therapy. 2023; 17: 39–53. https://doi.org/10.2147/DDDT.S385208

[30] Kim S, Chen J, Cheng T, Gindulyte A, He J, He S. PubChem 2025 update. Nucleic Acids Research. 2025; 53: D1516–D1525. https://doi.org/10.1093/nar/gkae1059

[31] Seeliger D, de Groot BL. Ligand docking and binding site analysis with PyMOL and Autodock/Vina. Journal of Computer-aided Molecular Design. 2010; 24: 417–422. https://doi.org/10.1007/s10822-010-9352-6

[32] Hildebrand PW, Rose AS, Tiemann JKS. Bringing Molecular Dynamics Simulation Data into View. Trends in Biochemical Sciences. 2019; 44: 902–913. https://doi.org/10.1016/j.tibs.2019.06.004

[33] Wang E, Sun H, Wang J, Wang Z, Liu H, Zhang JZH, et al. End-Point Binding Free Energy Calculation with MM/PBSA and MM/GBSA: Strategies and Applications in Drug Design. Chemical Reviews. 2019; 119: 9478–9508. https://doi.org/10.1021/acs.chemrev.9b00055

[34] Liu J, Ye T, Zhang Y, Zhang R, Kong Y, Zhang Y, et al. Protective Effect of Ginkgolide B against Cognitive Impairment in Mice via Regulation of Gut Microbiota. Journal of Agricultural and Food Chemistry. 2021; 69: 12230–12240. https://doi.org/10.1021/acs.jafc.1c05038

[35] Zou R, Liu Z, Wang P, Liu Y. Ginkgolide B binds to GPX4 and FSP1 to alleviate cerebral ischemia/reperfusion injury in rats. Toxicology and Applied Pharmacology. 2025; 495: 117237. https://doi.org/10.1016/j.taap.2025.117237

[36] Xu J, Wang KL, Cao ZY, Cao L, Wang ZZ, Xiao W. Antagonistic effect of ginkgolide homologues on PAF-induced platelet aggregation and neuroprotective effect. China Journal of Chinese Materia Medica. 2017; 42: 4716–4721. https://doi.org/10.19540/j.cnki.cjcmm.2017.0206 (In Chinese)

[37] Shang Q, Zhou X, Yang MR, Lu JG, Pan Y, Zhu GY, et al. Amide Derivatives of Ginkgolide B and Their Inhibitory Effects on PAF-Induced Platelet Aggregation. ACS Omega. 2021; 6: 22497–22503. https://doi.org/10.1021/acsomega.1c01682

[38] Cao Y, Yang L, Cheng H. Ginkgolide B Protects Against Ischemic Stroke *via* Targeting AMPK/PINK1. Frontiers in Pharmacology. 2022; 13: 941094. https://doi.org/10.3389/fphar.2022.941094

[39] Ivic L, Sands TTJ, Fishkin N, Nakanishi K, Kriegstein AR, Strømgaard K. Terpene trilactones from Ginkgo biloba are antagonists of cortical glycine and GABA(A) receptors. The Journal of Biological Chemistry. 2003; 278: 49279–49285. https://doi.org/10.1074/jbc.M304034200

[40] Guo Y, Mao M, Li Q, Yu X, Zhou L. Extracts of Ginkgo flavonoids and ginkgolides improve cerebral ischaemia-reperfusion injury through the PI3K/Akt/Nrf2 signalling pathway and multicomponent in vivo processes. Phytomedicine: International Journal of Phytotherapy and Phytopharmacology. 2022; 99: 154028. https://doi.org/10.1016/j.phymed.2022.154028

[41] Rhein V, Giese M, Baysang G, Meier F, Rao S, Schulz KL, et al. Ginkgo biloba extract ameliorates oxidative phosphorylation performance and rescues abeta-induced failure. PLoS ONE. 2010; 5: e12359. https://doi.org/10.1371/journal.pone.0012359

[42] Choi YK. Detrimental Roles of Hypoxia-Inducible Factor-1α in Severe Hypoxic Brain Diseases. International Journal of Molecular Sciences. 2024; 25: 4465. https://doi.org/10.3390/ijms25084465

[43] Chao AC, Chen CH, Wu MH, Hou BY, Yang DI. Roles of Id1/HIF-1 and CDK5/HIF-1 in cell cycle reentry induced by amyloid-beta peptide in post-mitotic cortical neuron. Biochimica et Biophysica Acta. Molecular Cell Research. 2020; 1867: 118628. https://doi.org/10.1016/j.bbamcr.2019.118628

[44] Ashok BS, Ajith TA, Sivanesan S. Hypoxia-inducible factors as neuroprotective agent in Alzheimer's disease. Clinical and Experimental Pharmacology & Physiology. 2017; 44: 327–334. https://doi.org/10.1111/1440-1681.12717

[45] Tang Z, Wang XL, Deng YX, Xiao Y, Xu JW, Wang L, et al. ABT263 Ameliorates Cellular Senescence, Aβ-Dependent Pathology and Cognitive Decline in Aged APP/PS1 Mice via Regulating PI3K/AKT/GSK-3β Pathways. Cell Biochemistry and Biophysics. 2025; 83: 3665–3676. https://doi.org/10.1007/s12013-025-01745-y

[46] Su W, Wang Y, Shao S, Ye X. Crocin ameliorates neuroinflammation and cognitive impairment in mice with Alzheimer's disease by activating PI3K/AKT pathway. Brain and Behavior. 2024; 14: e3503. https://doi.org/10.1002/brb3.3503

[47] Imiruaye OE, Perez IG, Carson BC, Crouzet C, Garcia J, Han D, et al. Spatiotemporal differential regulation of extrasynaptic GluN2B receptor subunits and PSA-NCAM in brain aging and Alzheimer's disease. Frontiers in Neuroscience. 2025; 19: 1649625. https://doi.org/10.3389/fnins.2025.1649625